Research Article | Vol. 29, No. 16 / 2 August 2021 / Optics Express 25100
Optics EXPRESS

Ppt level carbon monoxide detection based on light-induced thermoelastic spectroscopy exploring custom quartz tuning forks and a mid-infrared QCL

SHUNDA QIAO,[1] YUFEI MA,[1,*] YING HE,[1] PIETRO PATIMISCO,[2] ANGELO SAMPAOLO,[2] AND VINCENZO SPAGNOLO[2]

[1]National Key Laboratory of Science and Technology on Tunable Laser, Harbin Institute of Technology, Harbin 150001, China
[2]PolySense Lab – Dipartimento Interateneo di Fisica, University and Politecnico of Bari, Via Amendola 173, Bari, Italy
[*]mayufei@hit.edu.cn

Abstract: In this paper, we report on an ultra-highly sensitive light-induced thermoelastic spectroscopy (LITES)-based carbon monoxide (CO) sensor exploiting custom quartz tuning forks (QTFs) as a photodetector, a multi-pass cell and a mid-infrared quantum cascade laser (QCL) for the first time. The QCL emitting at 4.58 μm with output power of 145 mW was employed as exciting source and the multi-pass cell was employed to increase the gas absorption pathlength. To reduce the noise level, wavelength modulation spectroscopy (WMS) and second harmonic demodulation techniques were exploited. Three QTFs including two custom QTFs (#1 and #2) with different geometries and a commercial standard QTF (#3) were tested as photodetector in the gas sensor. When the integration time of the system was set at 200 ms, minimum detection limits (MDLs) of 750 part-per-trillion (ppt), 4.6 part-per-billion (ppb) and 5.8 ppb were achieved employing QTF #1 #2, and #3, respectively. A full sensor calibration was achieved using the most sensitive QTF#1, demonstrating an excellent linear response with CO concentration.

1. Introduction

Carbon monoxide (CO) is a colorless and odorless toxic air pollutant. The gas even with a low concentration level can be dangerous to human life. High concentrations of CO lead to reduced oxygen transport by hemoglobin and has health effects that include headaches, increased risk of chest pain for persons with heart disease and even death [1]. Therefore, an accurate and precise monitoring of CO in real-time is necessary. In daily life, CO is mainly produced by the incomplete combustion of carbonaceous materials, such as coal, petroleum, and natural gas. CO in the atmosphere will react with hydroxyl (OH) which can influence the concentration level of greenhouse gases and contribute to global warming. Motor-vehicle emissions are the primary source of CO in outdoor air in populated areas. Outdoor concentrations of CO tend to be higher in urban areas and to increase with the density of vehicles and miles driven. This means CO is also one of the important gases of the atmosphere environment monitor [2,3]. Besides, in the medical field, the detection of CO concentration exhaled by the human body can be used to diagnose asthma, diabetes, cystic fibrosis, and other diseases [4–6]. Therefore, it is significant to develop highly sensitive sensors for CO detection.

Laser absorption spectroscopy (LAS) is an effective trace gas detection technique. According to the different detection principles and configurations, many novel techniques based on LAS have been reported. Tunable laser absorption spectroscopy (TDLAS) is a common method which is based on direct laser absorption [7,8]. In TDLAS, a photoelectric detector is employed to measure the variation of the light intensity. A multi-pass cell is usually used to improve the

#434128 https://doi.org/10.1364/OE.434128
Journal © 2021 Received 14 Jun 2021; revised 9 Jul 2021; accepted 13 Jul 2021; published 21 Jul 2021

Optics EXPRESS

detection sensitivity by increasing the gas absorption pathlength. For many reported TDLAS based CO sensors, the detection limit was at part-per-million (ppm) or part-per-billion (ppb) levels [9,10]. In 2002, the quartz-enhanced photoacoustic spectroscopy (QEPAS) based gas sensing was firstly reported [11]. In QEPAS, a quartz tuning fork (QTF) is employed as an optoacoustic transducer, replacing the condenser microphone used in traditional photoacoustic spectroscopy (PAS) [12–15]. The high quality-factor and tiny size of QTFs are advantageous to improve the sensor performance and reduce the sensing volume [16–19]. Several CO-based QEPAS sensor have been reported so far. Y. Ma et al. reported on a portable sensitive CO gas sensor based on QEPAS technique exploiting a distributed feedback (DFB) diode laser emitting at 2.3 μm as excitation source [20]. With the addition of water vapor to accelerate the vibration translation rate of CO molecules, a minimum detection limit (MDL) of 9.1 ppm was achieved for a 1s integration time. S. Li et al. demonstrated an ultra-sensitive CO-QEPAS sensor exploiting a custom QTF with surface grooved and a QCL operating at 4.61 μm [21]. A CO MDL of 7 ppb at 300 ms integration time was achieved. Y. Ma et al. reported on a CO-Q EPAS sensor exploiting a high-power CW-DFB QCL, capable to emit at 4.61 μm up to 1000 mW of optical power and achieved an MDL of 1.5 ppb at 1 sec integration time [22].

Although TDLAS and QEPAS techniques are both sensitive methods to detect trace gases, there are some limitations. For TDLAS technique, it is difficult to obtain a photoelectric detector suitable for wavelength larger than 10 μm. Furthermore, the high price and big size of photoelectric detector limit its application. For QEPAS technique, the QTFs must be placed into the target analyte, which means it is a contact measurement method and is not applicable to detect corrosive gases or applied in some harsh conditions such as in combustion processes. In 2018, a novel technique based on light-induced thermoelastic spectroscopy (LITES) was proposed by Y. Ma et al [23]. In some publications, such technique was also called as quartz-enhanced photothermal spectroscopy (QEPTS). LITES avoids the above limitations of TDLAS and QEPAS. In LITES, a QTF was used as light detector and the laser beam is incident on the surface of QTF after being absorbed by the target gas sample. By modulating the laser intensity, the QTF heating will change periodically and this cause mechanical vibration of QTF according to the light-induced-thermoelastic conversion [23–26]. Such vibrations are enhanced when the QTF operates in resonance condition. Due to the piezoelectric effect, the QTF will generate an electrical signal which contains the information of gas concentration. Up to now, many gas detection techniques based on LITES have been reported [27–31]. A CO-LITES sensor was reported by Y. He et al. in 2019. With an integration time of 60 ms, an MDL of 470 ppb was achieved by using a multi-pass cell and a gas chamber containing a QTF with low pressure [32].

In this paper, we report on an ultra-highly sensitive CO-LITES sensor based on a mid-infrared QCL and custom QTFs. The output power of QCL was 145 mW at the target wavelength. A multi-pass cell with optical length of 10 m was employed to increase the gas absorption strength. Three QTFs including two custom QTFs (#1 and #2) with different geometries and a commercial standard QTF (#3) were used as the photodetector. Wavelength modulation spectroscopy (WMS) and the 2nd harmonic demodulation techniques were employed to reduce the background noise. Employing the optimum QTF, a part-per-trillion (ppt) level MDL for the CO detection was achieved.

2. Experimental setup

2.1. QCL characterization

The excitation source employed in this sensor system was a mid-infrared DFB-CW QCL with a central wavelength of 4.58 μm. By changing the driving current and operating temperature, the wavelength of QCL can be tuned to match a CO absorption line of R9 in R branch located at 4587.64 nm (2179.77 cm^{-1}), with a linestrength of $4.079 \cdot 10^{-19}$ $cm^{-1}/(molecule \cdot cm^{-2})$. The wavelength and output power of QCL as a function of driving current with different operating

Optics EXPRESS

temperatures are shown in Fig. 1(a) and Fig. 1(b), respectively. The temperature and driving current tuning coefficient of QCL wavelength were 0.42 nm/°C and 0.03 nm/mA, respectively. During the experiment, the laser temperature was set at 25 °C, and an output power of ~ 145 mW was achieved when the wavelength of the QCL matched the selected CO absorption line. At the output power of 50 mW, a 2D beam profile was obtained by utilizing a pyrocamera (Pyrocam IIIHR, Ophir) and is shown in the insert of Fig. 1(b). The laser beam profile resembles a slightly asymmetric Gaussian profile with small tails. The dimension of the beam is about 3.86 × 3.30 mm^2.

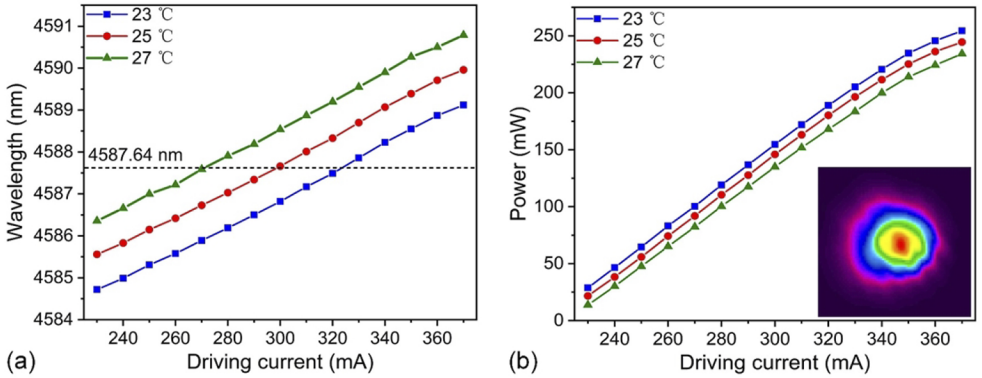

Fig. 1. (a)#Emission wavelength and (b) Output power of the employed QCL at different driving currents and three different operating temperatures.

2.2. Sensor configuration

A schematic of the LITES based CO detection system is depicted in Fig. 2(a). The laser beam emitted from QCL was incident into the multi-pass cell which contained two concave mirrors coated by gold with protective hafnium oxide (HfO_2) overcoat. The volume of the cell was 2.4 L and a wedge mirror made of calcium fluoride (CaF_2) was used as input window. There are two detachable small apertures set at the laser incident end of the multi-pass cell. When the entirely laser passed through the two small apertures, the laser was incident into the multi-pass cell with the optimum angle. After the adjustment, the two small apertures were removed to avoid blocking the reflected laser beam. With the optimum laser incident angle, the laser beam in the cell can achieve 34 times reflections, corresponding to a ~10.13 m optical length. The laser beam exiting from the multi-pass cell was focused on the surface of the QTF, acting as photodetector. Two custom QTFs (#1 and #2) were used in the experimental setup and for comparison, a commercial standard QTF (#3) was also tested. A picture of the employed QTFs is shown in Fig. 2(b). The surfaces of the commercial QTF and custom QTFs were coated with silver and gold layers, respectively. A mixture of 10 ppm CO balanced with nitrogen (N_2) was used as the target gas to investigate the performance of the sensor system. Two gas flow controllers with the uncertainty of ± 1% at full scale were employed to adjust the mixing ratio of CO and N_2, generating gas mixture with different CO:N_2 concentrations. For the three QTS, the laser beam was focused on the quartz surface close to the base of the prongs, where the highest LITES signal is expected [32]. The focal length of the lens was 30 mm. To reduce the background noise, wavelength modulation spectroscopy (WMS) and the second harmonic demodulation techniques were employed. A function generator provided a ramp wave for scanning the laser wavelength across the selected gas absorption line. A lock-in amplifier generated a sine wave used to modulate the laser wavelength and as reference signal for demodulation. For the WMS technique, the laser wavelength will across the gas absorption line twice in one period of the modulation by the sine wave. Therefore,

Optics EXPRESS

the frequency of modulated sine wave was set at half of the resonant frequency of QTF while the signal is demodulated at the resonance frequency. The detection bandwidth of the used lock-in amplifier was 390 mHz.

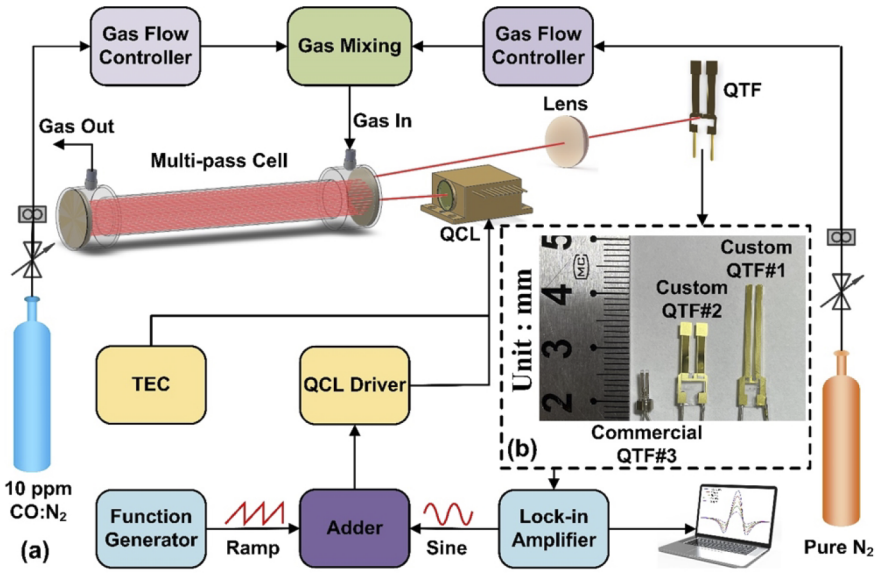

Fig. 2. (a) Schematic of the CO-LITES sensor with a mid-infrared QCL and a multi-pass cell. (b) The dimension diagram of the three QTFs. QCL: quantum cascade laser; QTF: quartz tuning fork; TEC: thermos-electric cooler.

3. Experimental results and discussions

The resonant frequencies of the three QTFs were firstly measured. The measured frequency response of the three QTFs is shown in Fig. 3. The detailed parameters for different QTFs are listed in Table 1.

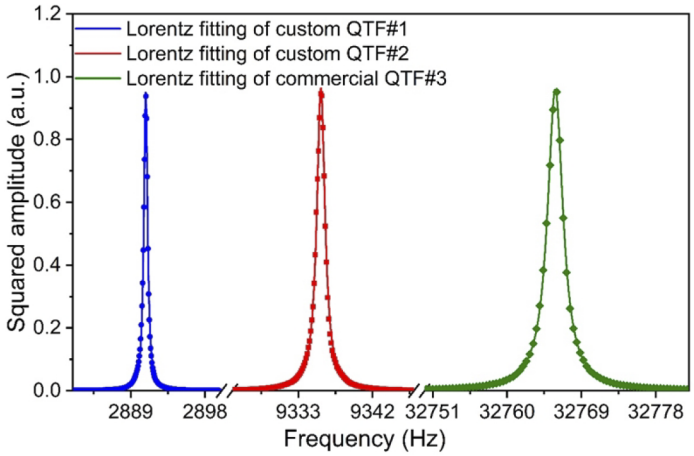

Fig. 3. Frequency response of custom QTF#1, custom QTF#2 and commercial QTF#3, respectively.

Optics EXPRESS

Table 1. Measured parameters for different QTFs.

QTF No.	Resonant frequency f (Hz)	Detection bandwidth (Hz)	Q factor
QTF#1	2890.8	0.53	5454
QTF#2	9335.7	1.21	7715
QTF#3	32766.8	2.29	14308

The data were normalized and fitted with a Lorentzian function. Resonant frequency (f) of 2890.8 Hz, 9335.7 Hz and 32766.8 Hz with the detection bandwidth of Δf_1=0.53 Hz, Δf_2=1.21 Hz and Δf_3=2.29 Hz were measured for QTF#1, QTF#2 and QTF#3, respectively. According to the formula of $Q = f/\Delta f$, the quality factor for three QTFs resulted $Q_1 = 5454$, Q_2=7715 and Q_3=14308, respectively.

In WMS technique, modulation depth is an important parameter which influences the amplitude of the detected signal significantly. Therefore, the current modulation depths of the system using the three different QTFs were optimized, respectively. The laser wavelength was locked at the gas absorption peak and the amplitude of the modulated sine wave was varied to identify the optimal current modulation depth. The 2f signal amplitude as a function of current modulation depth is shown in Fig. 4. It can be seen that for each QTF, the 2f signal reached the maximum when the current modulation depth was 15 mA, thereby resulting the optimum value for the sensor system.

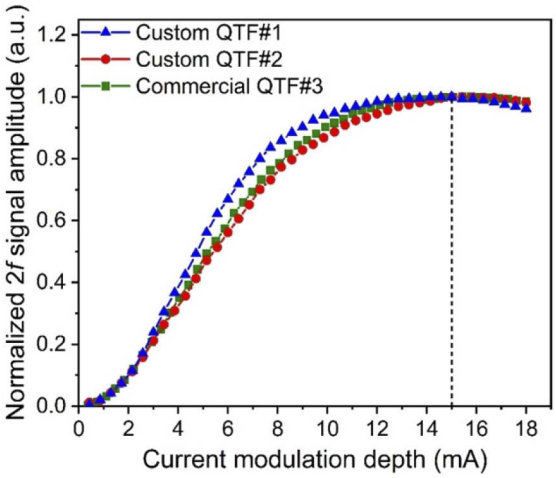

Fig. 4. 2f signal amplitude of CO-LITES sensor as a function of current modulation depth for the three different QTFs.

The 2f signals using the optimum values of modulation frequency and current modulation depth measured with the three QTFs are shown in Fig. 5. With an integration time of 200 ms, the 2f signal amplitude for the system with QTF#1, QTF#2 and QTF#3 resulted 28.89 mV, 10.18 mV and 5.17 mV, respectively. The front surface of custom QTFs is uncoated to allow laser transmission through the quartz, while the back surface is coated with gold film to back-reflect the laser. This special design enhanced the laser absorption for LITES [24,26]. Furthermore, a QTF with a small resonant frequency is beneficial to increase the energy accumulation in LITES. Therefore, QTF#1 provided the highest signal level.

Because QTF#1 had the strongest signal response, the sensor performance of gas concentration response was investigated with it in the following experiments. 10 ppm CO was diluted with pure N_2 by using two gas flow controllers to produce CO analyte with different concentrations. The 2f signal was measured with different CO concentrations and the results were shown in Fig. 6(a).

Optics EXPRESS

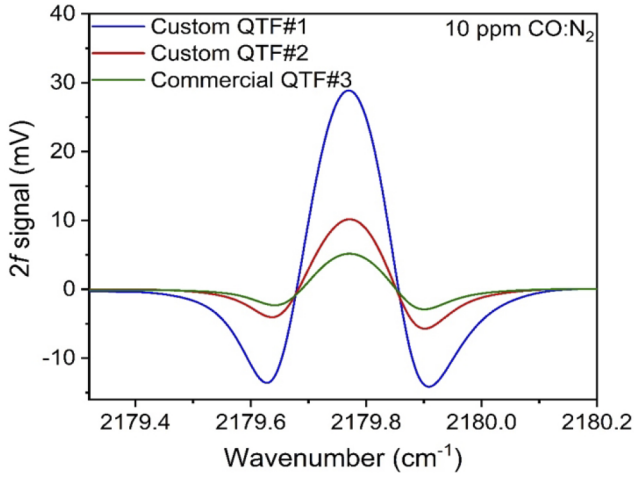

Fig. 5. 2*f* signal of CO-LITES sensor systems for the three different QTFs.

The signal peaks as a function of gas concentrations were displayed in Fig. 6(b). After using a linear fitting, the obtained R-square was 0.99, which proved the system has an excellent linear response of gas concentration.

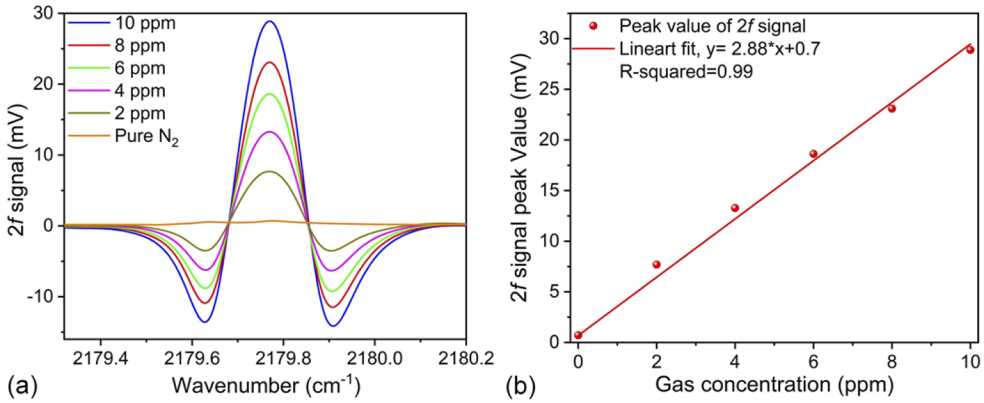

Fig. 6. (a) 2*f* signal with different gas concentrations when QTF#1 was used. (b) 2*f* signal peak values as a function of gas concentrations.

To evaluate the sensor performance of MDL, the noise levels of the three QTFs were measured when the multi-pass cell was filled with pure N_2 when the laser is locked on the selected CO absorption wavelength. The obtained results are depicted in Fig. 7, and the 1σ noise of the system using the three different QTFs resulted 2.16 μV, 4.69 μV and 2.98 μV for QTF#1, QTF#2 and QTF#3, respectively. The small offsets shown in Fig. 7 resulted from the effect of photo-thermoelastic energy conversion induced by laser absorption of QTFs [33]. Accordingly, the signal to noise ratio (SNR) resulted 13375, 2171 and 1735 for QTF#1, QTF#2 and QTF#3, respectively, which corresponds to an MDL of 750 ppt, 4.6 ppb and 5.8 ppb for the detection of CO gas.

Optics EXPRESS

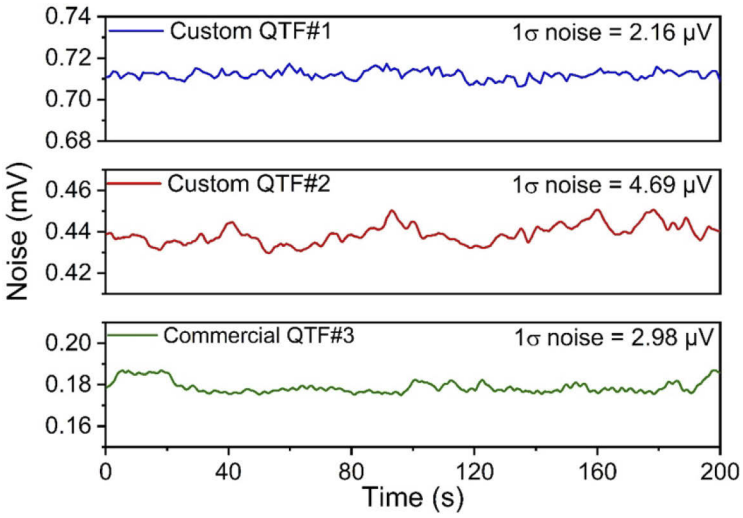

Fig. 7. Noise level of system for the three different QTFs.

4. Conclusions

In conclusion, an ultra-highly sensitive LITES based CO sensor with ppt level detection ability by using custom QTFs and a mid-infrared QCL was demonstrated in this paper. The wavelength of QCL was tuned to match a CO absorption line located at 4587.64 nm. When the operating temperature of QCL was set at 25 °C, the laser power was 145 mW at the target wavelength. A multi-pass cell with an optical length of 10 m was employed to increase the gas absorption length. WMS and the second harmonic demodulation techniques were adopted to reduce the background noise of the system. Two custom QTFs (#1 and #2) with low resonant frequency (<10 kHz) were used as the photodetector to improve the sensor performance. Moreover, a commercial standard 32.768 kHz QTF (#3) was also adopted for comparison. When the integration time was set at 200 ms, the MDL of the systems employing QTF#1, QTF#2 and QTF#3 were 750 ppt, 4.6 ppb and 5.8 ppb, respectively. The performance of the proposed CO sensor can be further improved by enclosing the QTF photodetector into a chamber at low pressure to further increase its quality factor and thereby its sensitivity level. Furthermore, QTF coated with other material can increase the light absorption to enhance its photo-thermoelastic energy conversion [34].

Funding. National Natural Science Foundation of China (61505041, 61875047, 62022032); Natural Science Foundation of Heilongjiang Province (YQ2019F006); Heilongjiang Provincial Postdoctoral Science Foundation (LBH-Q18052); Fundamental Research Funds for the Central Universities; THORLABS GmbH within the joint-research laboratory PolySense.

Disclosures. The authors declare no conflicts of interest.

Data availability. Data underlying the results presented in this paper are not publicly available at this time but may be obtained from the authors upon reasonable request.

References

1. J. J. Rose, L. Wang, Q. Xu, C. F. Mctiernan, S. Shiva, J. Tejero, and M. T. Galdwin, "Carbon monoxide poisoning: pathogenesis, management, and future directions of therapy," Am. J. Respir. Crit. Care Med. **195**(5), 596–606 (2017).
2. M. Khalil and R. A. Rasmussen, "Carbon monoxide in the earth's atmosphere: increasing trend," Science **224**(4644), 54–56 (1984).
3. S. Solomon, R. R. Garcia, J. J. Olivero, R. M. Bevilacqua, P. R. Schwartz, R. T. Clancy, and D. O. Muhleman, "Photochemistry and transport of carbon monoxide in the middle atmosphere," J. Atmos. Sci. **42**(10), 1072–1083 (1985).

Optics EXPRESS

4. L. Y. Wu and R. Wang, "Carbon monoxide: endogenous production, physiological functions, and pharmacological applications," Pharmacol. Rev. **57**(4), 585–630 (2005).
5. K. Zayasu, K. Sekizawa, S. Okinaga, S. Yamaya, T. Ohrui, and H. Sasaki, "Increased carbon monoxide in exhaled air of asthmatic patients," Am. J. Respir. Crit. Care Med. **156**(4), 1140–1143 (1997).
6. H. Okuyama, M. Yonetani, Y. Uetani, and H. Nakamura, "End-tidal carbon monoxide is predictive for neonatal non-hemolytic hyperbilirubinemia," Pediatr. Int. **43**(4), 329–333 (2001).
7. H. B. Lu, C. T. Zheng, L. Zhang, Z. W. Liu, Y. Zhang, and Y. D. Wang, "A remote sensor system based on TDLAS technique for ammonia leakage monitoring," Sensors **21**(7), 2448 (2021).
8. C. G. Li, L. Lei, C. T. Zheng, and F. K. Tittel, "Compact TDLAS based optical sensor for ppb-level ethane detection by use of a 3.34 μm room-temperature CW interband cascade laser," Sens. Actuators, B **232**, 188–194 (2016).
9. D. Thomazy, S. So, A. Kosterev, R. Lewicki, L. Dong, A. A. Sani, and F. K. Tittel, "Low-power laser-based carbon monoxide sensor for fire and post-fire detection using a compact herriott multipass cell," Proc. SPIE **7608**, 76080C (2010).
10. L. G. Shao, B. Fang, F. Zheng, X. B. Qiu, Q. S. He, J. L. Wei, C. L. Li, and W. X. Zhao, "Simultaneous detection of atmospheric CO and CH_4 based on TDLAS using a single 2.3 μm DFB laser," Spectroc. Acta. Pt. A-Molec. Biomolec. Spectr. **222**, 117118 (2019).
11. A. A. Kosterev, Y. A. Bakhirkin, R. F. Curl, and F. K. Tittel, "Quartz-enhanced photoacoustic spectroscopy," Opt. Lett. **27**(21), 1902–1904 (2002).
12. S. D. Qiao, Y. F. Ma, P. Patimisco, A. Sampaolo, Y. He, Z. T. Lang, F. K. Tittel, and V. Spagnolo, "Multi-Pass quartz-enhanced photoacoustic spectroscopy-based trace gas sensing," Opt. Lett. **46**(5), 977–980 (2021).
13. L. Hu, C. T. Zheng, M. H. Zhang, D. Yao, J. Zheng, Y. Zhang, Y. D. Wang, and F. K. Tittel, "Quartz-enhanced photoacoustic spectroscopic methane sensor system using a quartz tuning fork-embedded, double-pass and off-beam configuration," Photoacoustics **18**, 100174 (2020).
14. H. D. Zheng, Y. H. Liu, H. Y. Lin, B. Liu, X. H. Gu, D. Q. Li, B. C. Huang, Y. C. Wu, L. P. Dong, W. G. Zhu, J. Y. Tang, H. Y. Guan, H. H. Liu, Y. C. Zhong, J. B. Fang, Y. H. Luo, J. Zhang, J. H. Yu, Z. Chen, and F. K. Tittel, "Quartz-enhanced photoacoustic spectroscopy employing pilot line manufactured custom tuning forks," Photoacoustics **17**, 100158 (2020).
15. Y. Li, R. Z. Wang, F. K. Tittel, and Y. F. Ma, "Sensitive methane detection based on quartz-enhanced photoacoustic spectroscopy with a high-power diode laser and wavelet filtering," Opt. Lasers Eng. **132**, 106155 (2020).
16. J. P. Waclawek, H. Moser, and B. Lendl, "Compact quantum cascade laser based quartz-enhanced photoacoustic spectroscopy sensor system for detection of carbon disulfide," Opt. Express **24**(6), 6559–6571 (2016).
17. M. Mordmüller, M. Köhring, W. Schade, and U. Willer, "An electrically and optically cooperated QEPAS device for highly integrated gas sensors," Appl. Phys. B **119**(1), 111–118 (2015).
18. L. Dong, A. A. Kosterev, D. Thomazy, and F. K. Tittel, "QEPAS spectrophones: design, optimization, and performance," Appl. Phys. B **100**(3), 627–635 (2010).
19. Z. L. Li, Z. Wang, Y. Qi, W. Jin, and W. Ren, "Improved evanescent-wave quartz-enhanced photoacoustic CO sensor using an optical fiber taper," Sens. Actuators, B **248**, 1023–1028 (2017).
20. Y. F. Ma, G. Yu, J. B. Zhang, X. Yu, and R. Sun, "Sensitive detection of carbon monoxide based on a QEPAS sensor with a 2.3 μm fiber-coupled antimonide diode laser," J. Opt. **17**(5), 055401 (2015).
21. S. Li, L. Dong, H. Wu, A. Sampaolo, P. Patimisco, V. Spagnolo, and F. K. Tittel, "Ppb-level quartz-enhanced photoacoustic detection of carbon monoxide exploiting a surface grooved tuning fork," Anal. Chem. **91**(9), 5834–5840 (2019).
22. Y. F. Ma, R. Lewicki, M. Razeghi, and F. K. Tittel, "QEPAS based ppb-level detection of CO and N_2O using a high power CW DFB-QCL," Opt. Express **21**(1), 1008–1019 (2013).
23. Y. F. Ma, Y. He, Y. Tong, X. Yu, and F. K. Tittel, "Quartz-tuning-fork enhanced photothermal spectroscopy for ultra-high sensitive trace gas detection," Opt. Express **26**(24), 32103–32110 (2018).
24. S. Dello Russo, A. Zifarelli, P. Patimisco, A. Sampaolo, T. T. Wei, H. P. Wu, L. Dong, and V. Spagnolo, "Light-induced thermo-elastic effect in quartz tuning forks exploited as a photodetector in gas absorption spectroscopy," Opt. Express **28**(13), 19074–19084 (2020).
25. Y. F. Ma, "Recent advances in QEPAS and QEPTS based trace gas sensing: a review," Front. Phys. **8**, 268 (2020).
26. Y. F. Ma, Y. He, P. Patimisco, A. Sampaolo, S. D. Qiao, X. Yu, F. K. Tittel, and V. Spagnolo, "Ultra-high sensitive trace gas detection based on light-induced thermoelastic spectroscopy and a custom quartz tuning fork," Appl. Phys. Lett. **116**(1), 011103 (2020).
27. Y. F. Ma, Y. Q. Hu, S. D. Qiao, Y. He, and F. K. Tittel, "Trace gas sensing based on multi-quartz-enhanced photothermal spectroscopy," Photoacoustics **20**, 100206 (2020).
28. D. Pinto, H. Moser, J. P. Waclawek, S. D. Russo, P. Patimisco, V. Spagnolo, and B. Lendl, "Parts-per-billion detection of carbon monoxide: a comparison between quartz-enhanced photoacoustic and photothermal spectroscopy," Photoacoustics **22**, 100244 (2021).
29. Q. D. Zhang, J. Chang, Z. H. Cong, and Z. L. Wang, "Quartz tuning fork enhanced photothermal spectroscopy gas detection system with a novel QTF-self-difference technique," Sens. Actuators A. **299**, 111629 (2019).
30. S. D. Qiao, Y. He, and Y. F. Ma, "Trace gas sensing based on single-quartz-enhanced photoacoustic-photothermal dual spectroscopy," Opt. Lett. **46**(10), 2449–2452 (2021).

Optics EXPRESS

31. Y. Q. Hu, S. D. Qiao, Y. He, Z. T. Lang, and Y. F. Ma, "Quartz-enhanced photoacoustic-photothermal spectroscopy for trace gas sensing," Opt. Express **29**(4), 5121–5127 (2021).
32. Y. He, Y. F. Ma, Y. Tong, X. Yu, and F. K. Tittel, "Ultra-high sensitive light-induced thermoelastic spectroscopy sensor with a high Q-factor quartz tuning fork and a multipass cell," Opt. Lett. **44**(8), 1904–1907 (2019).
33. Z. T. Lang, S. D. Qiao, Y. He, and Y. F. Ma, "Quartz tuning fork-based demodulation of an acoustic signal induced by photo-thermo-elastic energy conversion," Photoacoustics **22**, 100272 (2021).
34. C. G. Lou, H. J. Chen, X. T. Li, X. Yang, Y. Zhang, J. Q. Yao, Y. F. Ma, C. Chang, and X. L. Liu, "Graphene oxide and polydimethylsiloxane coated quartz tuning fork for improved sensitive near- and mid-infrared detection," Opt. Express **29**(13), 20190–20204 (2021).